Analysis of Multiple Segmented Transmitters Design in Dynamic Wireless Power Transfer for Electric Vehicles Charging

Xiaolin Mou and Hongjian Sun

Multiple segmented transmitters rail for dynamic wireless power transfer (DWPT) electric vehicles (EVs) charging can supply high power transfer efficiency (PTE). Previous research discussed the vehicles' speed is a key factor that can affect the design of the rail (especially, the distance between two neighbouring segmented transmitters T) to maximize the system's PTE. However, this paper finds out not the vehicle's speed but the size of the transmitter rail can affect the design of T for optimizing the PTE.

Introduction: Although Electric Vehicles (EVs) have been widely accepted in many countries, EVs charging has become a challenge for facilitating long-lasting development of EVs. EVs charging technologies can be classified as conventional plug-in charging and wireless EVs charging. Compared to plug-in EVs charging, wireless EVs charging makes the car charged automatically and conveniently.

Wireless EVs charging technologies can be further divided into static charging and dynamic charging. In a dynamic wireless EVs charging system, EVs can be continuously charged in a dedicated charging lane using multiple coils embedded in the road [1]. EVs can therefore carry smaller batteries and even without batteries. Currently, many research groups are working on dynamic wireless power transfer (DWPT). Korea Advanced Institute of Science and Technology developed an innovative on-road dynamic wireless charging technology for electrical vehicles (OLEV) which can implement fast charging in the range of 100 KW of power capacity [2]. Staff in Oak Ridge National Laboratory implemented an experimental campus GEM EV with a WPT secondary coil, and the charging line composed of a number of roadway embedded coils [3].

In the literature, there are two types of transmitter rail design: long transmitter rail, and multiple segmented transmitters rail, as shown in Fig. 1. The long transmitter rail provides steady power flow for certain distance. But its power transfer efficiency (PTE) is lower than that of using the segmented transmitters rail [4, 5]. Lu *et al.* [6] proposed multiple rectangular transmitter coils at the primary side as the transmitter rail, with a complete system design and experiment setup. However, how to design the distance between the segmented transmitters has not been studied. O. Smiai *et al.* discussed the speed limit is necessary with the charging pad design in order to maximize the PTE [7]. However, we find out the vehicle's speed cannot affect the design of T for maximizing the PTE. In this paper, we propose a new theoretic model for addressing the different cases of multiple segmented transmitters rail design in DWPT EVs charging. Simulation results show that not the vehicle's speed but the size of the transmitter rail can affect the design of T for optimizing the PTE.

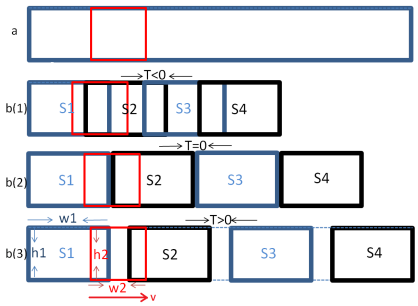

Fig. 1 *Top: long transmitter rail, and bottom three sub-figures: multiple segmented transmitters rail design using same receiver (red coil)*

System Model: As shown in Fig. 1, the blue coil and black coil are the adjacent segmented transmitters. The length of the segmented transmitter is w_1, and the width of the segmented transmitter is h_1. The red coil is the receiver which is fixed in the car. It is a rectangular coil, the length of the receiver coil is w_2 and the width h_2 of receiver is the same as transmitter width h_1. When the receiver coil arrives at the transmitter, the previous transmitter will be switched off at the same time. The distance between two neighbouring segmented transmitters is T where $T<0$ means two segmented transmitters are overlapped; $T=0$, means two segmented transmitters are next to each other; $T>0$ indicates there is a gap between two segmented transmitters.

Assuming the speed of the vehicle is v km/h, shown as Fig. 1. The time of the receiver coil enters into the first segmented transmitter is $t=t_0$, the horizontal coordinate of the receiver coil center point at $-\frac{1}{2}w_1-\frac{1}{2}w_2$. The receiver coil arrives at the second segmented transmitter in time $t=t_1$, the horizontal coordinate of the receiver coil center point is $T+\frac{1}{2}w_1-\frac{1}{2}w_2$. So the horizontal displacement of the receiver coil is $T+w_1$, and the total time is t. The horizontal coordinate of the receiver coil center point x_0 can be written as:

$$x_0 = v\cdot t - \frac{1}{2}\cdot w_1 - \frac{1}{2}\cdot w_2, t\in(0,\frac{T+w_1}{v}) \tag{1}$$

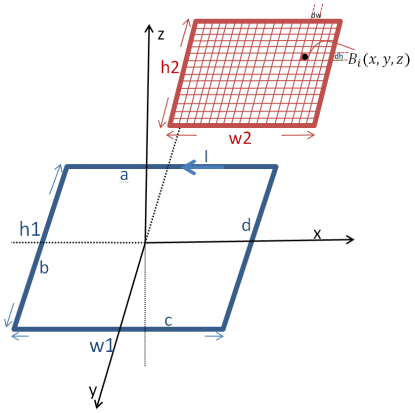

Fig. 2. Structure of two resonant coils

Proposed Method: Fig. 2 is a schematic illustration of two resonant coils. The blue rectangular coil is the transmitter coil, and the red rectangular coil is the receiver coil. The transmitter coil has four parts (line a, line b, line c and line d). The transmitter coil with N_1 turns is w_1 in length and h_1 in width, respectively. The receiver coil with N_2 turns is w_2 in length and h_2 in width, respectively. $\mathbf{I}$ is the current in the transmitter coil. The receiver coil is subdivided to many little rectangles and each subdivision with d_w length and d_h width. B_i is the subdivision magnetic field density in each subdivision [8], and only z direct flux can affect the mutual inductance. Subsequently B_i can be written by:

$$B_i = B_{zi}(a)+B_{zi}(b)+B_{zi}(c)+B_{zi}(d) \tag{2}$$

where $B_{zi}(a)$, $B_{zi}(b)$, $B_{zi}(c)$, and $B_{zi}(d)$ denote the magnetic field density due to current in lines a, b, c, d, respetively. According to Biot-Savart's Law, they can be written by:

$$B_{zi}(a) = \frac{\mu_0 N_1 \mathbf{I}}{4\pi}\cdot\frac{y+h_1/2}{(y+h_1/2)^2+z^2} \cdot\left[\frac{x+w_1/2}{\sqrt{(y+h_1/2)^2+z^2+(x+w_1)^2}}-\frac{x-w_1/2}{\sqrt{(y+h_1/2)^2+z^2+(x-w_1)^2}}\right] \tag{3}$$

$$B_{zi}(b) = \frac{\mu_0 N_1 \mathbf{I}}{4\pi}\cdot\frac{x+w_1/2}{(x+w_1/2)^2+z^2} \cdot\left[\frac{y+h_1/2}{\sqrt{(y+h_1/2)^2+z^2+(x+w_1)^2}}-\frac{y-h_1/2}{\sqrt{(y-h_1/2)^2+z^2+(x+w_1)^2}}\right] \tag{4}$$

$$B_{zi}(c) = \frac{\mu_0 N_1 \mathbf{I}}{4\pi}\cdot\frac{-(y-h_1/2)}{(y-h_1/2)^2+z^2} \cdot\left[\frac{x+w_1/2}{\sqrt{(y-h_1/2)^2+z^2+(x+w_1)^2}}-\frac{x-w_1/2}{\sqrt{(y-h_1/2)^2+z^2+(x-w_1)^2}}\right] \tag{5}$$

$$B_{zi}(d) = \frac{\mu_0 N_1 \mathbf{I}}{4\pi}\cdot\frac{-(x-w_1/2)}{(x-w_1/2)^2+z^2} \cdot\left[\frac{y+h_1/2}{\sqrt{(y+h_1/2)^2+z^2+(x-w_1)^2}}-\frac{y-h_1/2}{\sqrt{(y-h_1/2)^2+z^2+(x-w_1)^2}}\right] \tag{6}$$

where μ_0 is the permeability of free space. x, y and z are the center

point's coordinates of an arbitrary subdivision. The mutual inductance M_{12} can be written as the sum of each subdivision [8]:

$$M_{12} = \frac{N_1 N_2 d_w d_h}{\mathbf{I}} \sum_{i=1}^{N_w = w_2/d_w} \sum_{i=1}^{N_h = h_2/d_h} |B_i| \tag{7}$$

According to [9], the power transfer efficiency (PTE) η can be written by:

$$\eta = \frac{\frac{\Gamma_W}{\Gamma_Q}\frac{K^2}{\Gamma_P \Gamma_Q}}{(1+\frac{\Gamma_W}{\Gamma_Q})^2 + (1+\frac{\Gamma_W}{\Gamma_Q})\frac{K^2}{\Gamma_P \Gamma_Q}} \tag{8}$$

where

$$\Gamma_P = \frac{R_P}{2L_P}, \Gamma_Q = \frac{R_Q}{2L_Q}, K = \frac{M_{12}\omega}{2\sqrt{L_P L_Q}} \tag{9}$$

The subscripts P and Q denote the primary resonant coil and the secondary resonant coil. W denote the load. Γ is the intrinsic decay rate, and it depends on the resistance and self-inductance of the resonant coils. R_P is the total resistance of the primary resonant coil, L_P is the self-inductance of the primary resonant coil. R_Q is the total resistance of the secondary resonant coil, L_Q is the self-inductance of the secondary resonant coil. K is the coupling coefficient between the two resonant coils. The PTE η can be maximized when $\Gamma_W = \Gamma_Q\sqrt{1+(K^2/\Gamma_P\Gamma_Q)}$, and η can be rewritten by:

$$\eta = \frac{\sqrt{1+\frac{K^2}{L_P L_Q}} - 1}{\sqrt{1+\frac{K^2}{L_P L_Q}} + 1} \tag{10}$$

For convenience, we use j as a subscript to denote two values: $j = P$ means the primary resonant coil, and $j = Q$ represents the secondary resonant coil. The parameters of resonant coils can be given by [10]:

$$L_j = \frac{\mu_0 \mu_r}{\pi}\left[w \cosh^{-1}\frac{h}{2a} - h\cosh^{-1}\frac{w}{2a}\right] \tag{11}$$

$$R_j = \frac{w+h}{a\pi}\sqrt{\frac{2f\pi\mu_0\mu_r}{2\sigma}} + 20\left\{\left[\frac{2f\pi}{c}\right]^2 \cdot w \cdot h\right\}^2 \tag{12}$$

where μ_r is the relative permeability, w is the length of the rectangular coil, and h is the width of the rectangular coil. a is the wire radius of the coil. c is the speed of light, σ is the conductivity of the conductor and f is the resonant frequency. $L_j$and R_j are the self-inductance and the resistance of resonant coils, respectively.
Overall, we use the following algorithm to calculate the system PTE.

Algorithm 1

Input:

1: Set all parameters' value w_1, w_2, h_1, h_2, μ_0, μ_r, a, f, σ;
2: Substitute $x = x_0$, y, z into the equation (2);
3: Substitute the resultant B_i of (2) into the equation (7), then get the mutual inductance M_{12};
4: Set $w = w_1$, $h = h_1$, and substitute them into (11), (12) to calculate L_P, R_P;
5: Set $w = w_2$, $h = h_2$, and substitute them into (11), (12) to calculate L_Q, R_Q;
6: Substitute L_P, L_Q, R_P, R_Q, M_{12} into (9) to get Γ_P, Γ_Q, K for calculating PTE using equation (8);

Output:

η;

Results: Fig. 3 shows the relation between PTE and two neighbouring segmented transmitters distance T, when the speed v increases from 0 km/h to 100 km/h. It can be seen when the sizes of transmitter rail and receiver are fixed, no matter what the vehicle's speed v is, the values of the PTE are same. The vehicle's speed v can not affect the design of the distance T to optimize the PTE.

Fig. 4 shows the relation between PTE and T when the vehicle's speed v is 30km/h. The difference between them is the size of transmitter rail. Red line (a) serves as the benchmark with the length w_1= 1.6m, the width h_1= 0.3m. For blue line (b), the length w_1 is same, but the width h_1

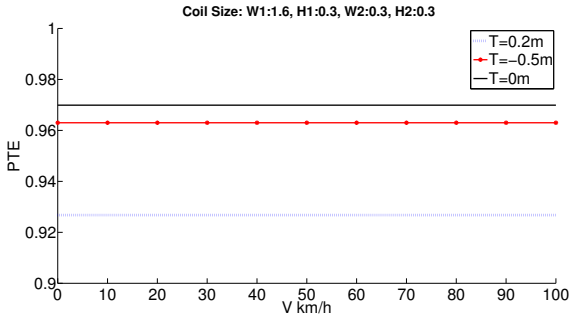

Fig. 3. The relation between PTE and T in different v

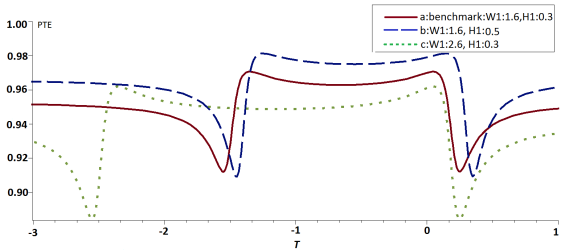

Fig. 4 *The relation between PTE and T in different size of segmented transmitters*

is bigger. The average PTE is higher than that of the benchmark. The width h_1 of green line (c) is same as the benchmark, but the length w_1 is longer. The average PTE is lower than that of the benchmark. In a word, the size of the transmitter rail can affect the design of the distance T for optimizing the PTE.

Conclusion: This paper has modeled multiple segmented transmitters' design in DWPT EVs charging. Based on the proposed theory and simulation results, the vehicle's speed v is not a determinant factor of T design. The size of the transmitter rail can affect the design of T for optimizing the PTE. In the future work, we will use this theory to choose an optimal distance between the neighbouring transmitter T that maximizes the PTE for EVs charging.

Xiaolin Mou and Hongjian Sun (*School of Engineering and Computing Sciences, University of Durham, UK*)

E-mail: hongjian.sun@durham.ac.uk

References

1 X. Mou *et al.*, "Energy Efficient and Adaptive Design for Wireless Power Transfer in Electric Vehicles," *IEEE Transactions on Industrial Electronics*, PP(99), pp.1-1, 2017.
2 I. S. Suh and J. Kim, "Electric vehicle on-road dynamic charging system with wireless power transfer technology," in *Proc. IEEE IEMDC*, Chicago, IL, 2013, pp. 234-240.
3 J. M. Miller *et al.*, "ORNL Experience and Challenges Facing Dynamic Wireless Power Charging of EV's," *IEEE Circuits and Systems Magazine*, pp. 40-53, Second quarter 2015.
4 K. Song *et al.*,"Wireless power transfer for running EV powering using multi-parallel segmented rails," in *Proc. IEEE WoW*, Daejeon, 2015, pp. 1-6.
5 K. K. Ean *et al.*, "Two-transmitter wireless power transfer with LCL circuit for continuous power in dynamic charging," in *Proc. IEEE WoW*, Daejeon, 2015, pp. 1-6.
6 F. Lu *et al.*, "A Dynamic Charging System with Reduced Output Power Pulsation for Electric Vehicles," *IEEE Transactions on Industrial Electronics*, 63(10), pp. 6580-6590, 2016.
7 O. Smiai *et al.*,"Information and Communication Technology Research Opportunities in Dynamic Charging for Electric Vehicle," in *Proc. 2015 Euromicro Conference on DSD*, Funchal, 2015, pp.297-300.
8 J. Kim *et al.*, "Efficiency of magnetic resonance WPT with two off-axis self-resonators," in *Proc. IEEE IMWS*, Uji, Kyoto, 2011, pp. 127-130.
9 Andre Kurs *et al.*, "Wireless Power Transfer via Strongly Coupled Magnetic resonances," *Science express*, pp. 83-86, June 2007.
10 Warren L. Stutzman, Thiele, Gary A. *"Antenna Theory and Design,"* John Wiley and Sons, 2007.